MDPI

Article

Interfacial Reactions between Mg-40Al and Mg-30Y Master Alloys

Jiahong Dai [1,*], Bin Jiang [2,*], Hongmei Xie [1] and Qingshan Yang [3]

[1] College of Materials Science and Engineering, Yangtze Normal University, Chongqing 408100, China; xhm1983@126.com

[2] State Key Laboratory of Mechanical Transmissions, College of Materials Science and Engineering, Chongqing University, Chongqing 400044, China

[3] School of Metallurgy and Materials Engineering, Chongqing University of Science and Technology, Chongqing 401331, China; qsyang@cqu.edu.cn

[*] Correspondence: daijiahong@yznu.edu.cn (J.D.); jiangbinrong@cqu.edu.cn (B.J.);
Tel.: +86-159-0236-1594 (J.D.); +86-135-9419-0166 (B.J.)

check for
updates

Abstract: Interfacial reactions between Mg-40Al and Mg-30Y master alloys were investigated at intervals of 25 °C in the 350–400 °C by using a diffusion couple method. Noticeable reaction layers were formed at the interfaces of the diffusion couples. The concentration profiles of the reaction layers were characterized. The diffusion path of the diffusion couple at 400 °C is constructed on the Mg-Al-Y ternary isothermal temperature phase diagram. The phases of the reaction layer were characterized by X-ray diffraction. The interfacial reaction thermodynamics of diffusion couples were studied. These results indicate that Al_2Y is the only new formed intermetallic phase in the reaction layers. The growth constants of the reaction layers were calculated. In the reaction layer II, the integrated interdiffusion coefficients of Al are higher than Y, the diffusion activation energy of Y is higher than that of Al.

Keywords: magnesium alloys; interface reaction; diffusion; intermetallic phases

1. Introduction

Magnesium alloys are important structural materials for automotive, aircraft, and aerospace lightweighting, due to their lower densities compared with steel and aluminum [1,2]. Currently, Mg-Al alloys such as AM60 and AZ91 are the most widely used commercial magnesium alloys. However, the applications of Mg-Al alloys are limited to room or near room-temperature because of inferior creep resistance and poor tensile properties at elevated temperatures above 120 °C. Adding Y to precipitate intermetallic phases in Mg-Al alloys is an efficient method to refine grain and improve the mechanical properties [3–7]. Therefore, a complete knowledge of the precipitation of intermetallic phases for the Mg-Al-Y system is crucial to a better understanding the role of Y in Mg-Al alloys.

In recent years, a lot of studies have been carried out on the in-situ formation of Al_2Y in Mg-Al alloys by adding a Y element [3–6]. Al_2Y is a very promising grain refiner. The Al_2Y phase transformation temperatures during solidification process were determine by thermal analysis combined with microstructural and EDX analysis. The nucleation crystallography and wettability of Al_2Y on the Mg grains have been investigated. However, no systematic diffusion kinetics studies have been performed for the Mg-Al-Y ternary system so far.

In recent decades, there have been thermodynamic and phase diagram studies on the Mg-Al-Y alloy systems. Shakhshir et al. [8] have established the Mg-Al-Y ternary thermodynamic model based on the extrapolation of the Mg-Al, Al-Y, Mg-Y binary subsystems by the CALPHAD approach.

The thermodynamic properties and the calculated phase diagrams are consistent with the literature. Huang et al. [9] have calculated the excess free-energy, enthalpies of formation, excess entropies and activity values of all components of Mg-Al-Y ternary alloy via the Miedema formation enthalpy model. The results show that enthalpies of formation, excess free-energy and excess entropies of the ternary alloy are negative in the whole content range. Dri et al. [10] presented Mg-Al-Y system isothermal sections between 300–500 °C for a vertical section at 80 wt % Mg. Zar et al. [11] and Odi et al. [12] constructed an isothermal section at 400 °C and confirmed the existence of a ternary compound Al₄MgY. In addition, Das et al. [13,14] have researched diffusion kinetic in the Mg-Al and Mg-Y systems. The impurity diffusion coefficients of Al and Y in Mg were determined. The interdiffusion coefficients and growth constants of the intermetallic phases were calculated. However, interfacial reactions and systematic diffusion kinetics studies in Mg-Al-Y systems are not fully reported. Therefore, studies are required to evaluate the interdiffusion interactions of elements and intermetallic phases formation in the interfacial reactions between Mg-Al and Mg-Y.

In this article, the interfacial reactions of (Mg-40Al)/(Mg-30Y) master alloys have been investigated at temperatures of 350–400 °C by diffusion couple method. The formation of the intermetallic phases at the interface of diffusion couples has been studied. The growth constants of the reaction layers have been analyzed by appropriate theories. The interdiffusion coefficients of Al and Y in the diffusion reaction lays have been determined.

2. Analytical Framework for Diffusion

2.1. Growth of Reaction Layers

The growth constants of the reaction layers were determined using a parabolic trend with time due to the diffusion-controlled process. The growth constant, k, can be calculated by:

$$x = \sqrt{kt} \tag{1}$$

where the thickness of reaction layer is x, and the annealing time is t. An Arrhenius relationship:

$$k = k_0 \exp\left(\frac{-Q}{RT}\right) \tag{2}$$

where the k_0 is pre-exponential factor, R is the gas constant, Q is the activation energy, and the annealing temperature is T.

2.2. Interdiffusion

Interdiffusion flux for each component was calculated according to the method proposed by Dayananda [15]:

$$\widetilde{J_i} = \frac{1}{2t} \int_{C_i^{-\infty}}^{C_i(x)} (x - x_0) dC_i, \, (i = Mg, Al, Y) \tag{3}$$

where $C_i(x)$ is the concentration of i, and t is the anneal time, and x_0 is the location of the Matan plane. For each reaction layer, the integrated interdiffusion coefficient $\widetilde{D}_i^{Int, \, layer}$ is calculated by the cumulative interdiffusion fluxes of individual components:

$$\widetilde{D}_i^{Int, \, layer} = \int_{x_1}^{x_2} \widetilde{J_i}(x) dx, \, (i = Mg, Al, Y) \tag{4}$$

where x_1 and x_2 are the position correspond to the intermetallic phase boundaries.

While the average effective interdiffusion coefficient, $\widetilde{D}_i^{eff}$, of each relevant reaction layer is calculated by [16]:

$$\widetilde{D}_i^{\text{eff}} = \frac{\int_{x_1}^{x_2} \widetilde{J}_i(x)dx}{\Delta C_i}, (i = Mg, Al, Y) \tag{5}$$

where ΔC_i is the difference of solute concentration at the end of i reaction layer.

3. Experimental

The terminal alloys of the diffusion couples were prepared from commercial Mg-40Al (Mg-40 wt % Al) and Mg-30Y (Mg-30 wt % Y) master alloy. The Mg-40Al master alloy is brittle and fragile, and its melting point (460 °C) is lower than that of Mg-30Y master alloy (595 °C). It is not feasible to make solid diffusion couples by the jig method. So a solid–liquid contact method was employed to produce the (Mg-40Al)/(Mg-30Y) diffusion couples. The method of preparing the (Mg-40Al)/(Mg-30Y) diffusion couples are the same as the previous works [17–19]. The Mg-40Al master alloy was melted in a crucible. Then, a piece of Mg-30Y master alloy with surface oxide removed was immediately submerged into Mg-40Al master alloy melt, and the crucible was taken from the furnace. An intimate contact between Mg-40Al and Mg-30Y master alloys was formed during solidification and the diffusion couple samples were obtained. Then the diffusion couples were isothermally heat-treated in a resistance furnace. The diffusion couples were carried out 350, 375 and 400 °C for 24, 48 and 72 h, respectively. Water-quenching after annealing is completed.

The diffusion couple samples were ground using 200–1000 emery papers. The microstructure of the cross-section was observed by scanning electron microscopy (SEM, TESCAN VEGA 2, TESCAN Co., Brno, Czech). Concentrations of Mg, Al and Y at the interfaces of diffusion couples were determined by energy dispersive spectroscopy (EDS, Oxford Inca, Oxford Instrument Technology Co., Ltd., Oxford, UK). Each EDS result is the average concentration of the elements for 5 μm × 150 μm rectangular map scanning, and the step length of the scanning is 5 μm. The intermetallic phases in the reaction layers were determined by X-ray diffractometer (XRD, D/MAX-2500PC, Dandong Fangyuan Instrument Co., Ltd., Dandong, China) and EDS. The thickness of the reaction layer is obtained by averaging the thickness of 10 random position measurement of the reaction layer.

4. Results and Discussion

4.1. Interfaces Microstructure

Typical back-scattered electron (BSE) micrographs of the cross-section for (Mg-40Al)/(Mg-30Y) diffusion couples annealing at 350, 375 and 400 °C for 24, 48 and 72 h, respectively, shown in Figure 1. As is seen in these micrographs, it is found that reaction layers are formed at the interfaces of diffusion couples. The intermetallic phases are formed in the reaction layers, and the reaction layer has obvious sub-layers. Thicknesses of the reaction layers increases with the increase in annealing temperature and time. As shown in Figure 1g, the sub-layer with a darker contrast located on the Mg-40Al matrix is named as layer I, and the intermetallic compound sub-layer with a brighter contrast located on the Mg-30Y matrix is named as layer II. As shown in Figure 1i, most of the newly formed intermetallic phases in the reaction layer distribute along the morphology of $Mg_{24}Y_5$ before diffusion in region 1. However, the morphology of the newly formed intermetallic phases near the Mg-30Y matrix is filamentous in region 2. In region 3, a dark stripe is formed at the end of the reaction layer near the Mg-30Y matrix.
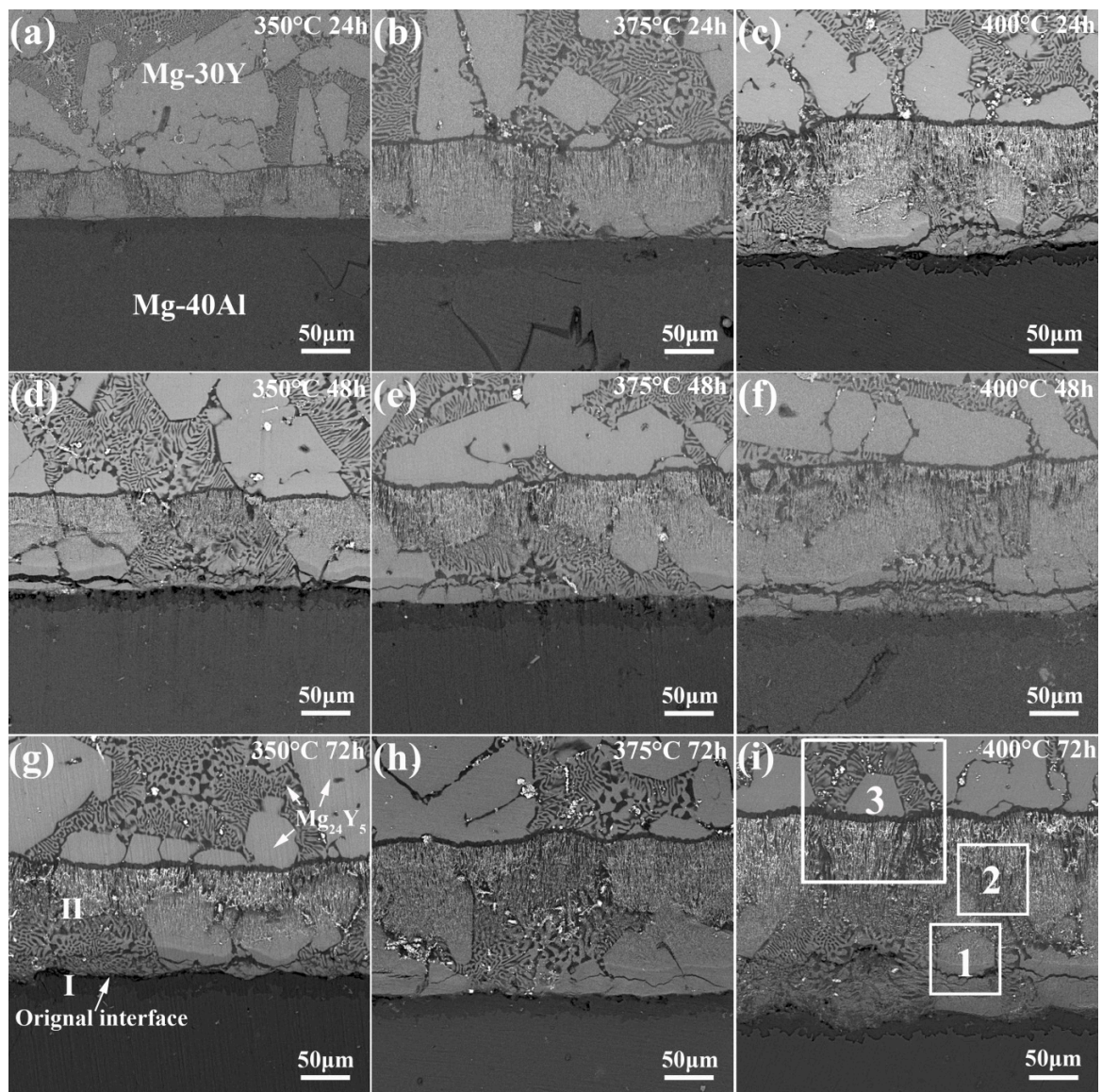
Figure 1. Back-scattered electron (BSE) micrographs of the diffusion couples annealing at 350, 375 and 400 °C for 24, 48 and 72 h. (**a**) at 350 °C, (**b**) at 375 °C and (**c**) at 400 °C for 24 h; (**d**) at 350 °C, (**e**) at 375 °C and (**f**) at 400 °C for 48 h; (**g**) at 350 °C, (**h**) at 375 °C and (**i**) at 400 °C for 72 h.

4.2. Concentration Profiles at Interfaces

Figure 2 shows the concentration profiles that were performed across the reaction lays of diffusion couples annealing at 350, 375 and 400 °C for 72 h, respectively. It is found that Y in Mg-30Y matrix hardly diffused into Mg-40Al matrix, but Al in Mg-40Al matrix diffused into Mg-30Y matrix. The concentration of Al in the reaction layers sharply falls from about 36 at.% to about 10 at.%, the concentration is essentially constant in the reaction layer I. then rises about 25 at.% when entering layer II, and finally decrease gradually are shown Figure 2a,c. Therefore, the sub-layer I is Al depletion compared, which is mainly Mg(Al) solid solution. The Al-Y intermetallic phases are formed when Al from Mg-40Al matrix diffused into Mg-30Y matrix. There is no significant fluctuation in the concentration of Y element in the sub-layer II. The result showed that Al and Y diffused differently in Mg.
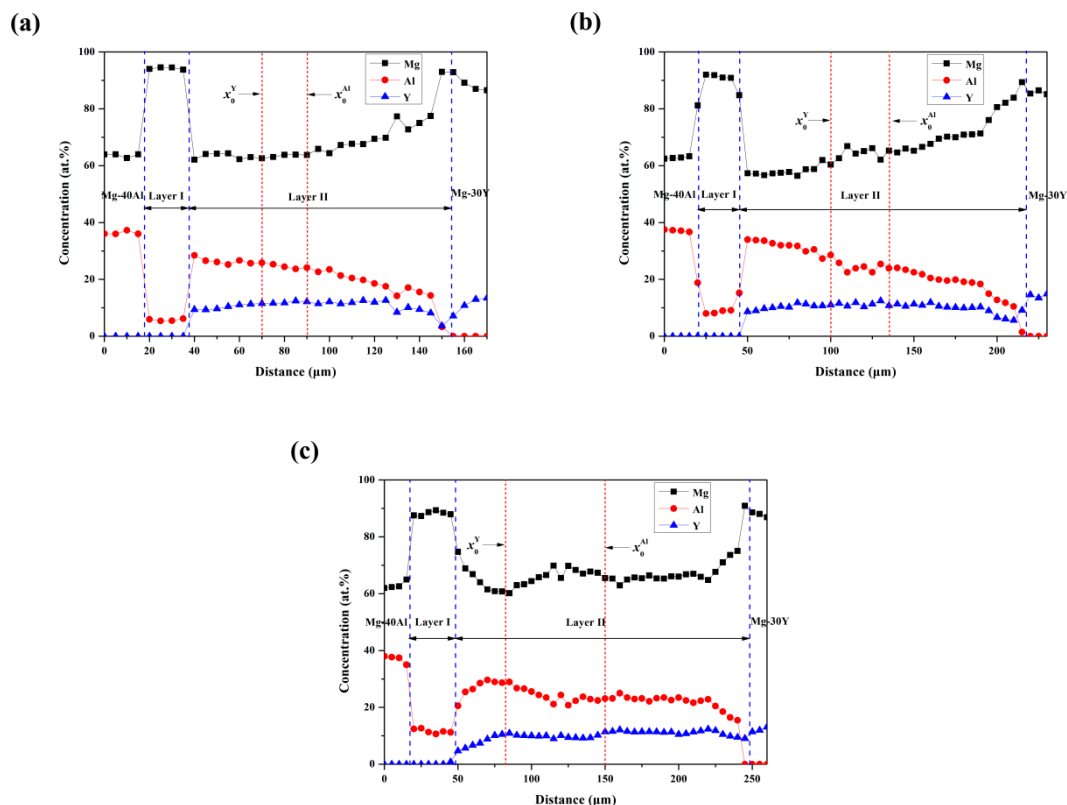
Figure 2. Concentration profiles Mg, Al and Y on the cross-section along the direction of diffusion for the diffusion couples annealed for 72 h at temperatures of (**a**) 350, (**b**) 375 and (**c**) 400 °C, respectively. x_0^{Al} and x_0^{Y} is the location of Matano plane for Al and Y, respectively.

4.3. Diffusion Path

The microstructure prediction of the diffusion process and the qualitative information on the relative diffusion behavior of the components can be realized by diffusion path. Any time on the concentration curve in the diffusion process can be mapped to a ternary isotherm [20,21]. Mg-Al-Y ternary isothermal temperature phase diagram of 400 °C has been determined [22]. Figure 3 shows the concentration curve is mapped onto Mg-Al-Y ternary phase diagram as diffusion path at 400 °C for 72 h. As shown in Figure 3b, the phase regions through which the diffusion path are as follow: Mg-40Al (terminal alloy) → Al_2Y + $\gamma(Mg_{17}Al_{12})$ + (Mg) → Al_2Y + (Mg) → Al_2Y + (Mg) + $Mg_{24}Y_5$ → Mg-30Y (terminal alloy). These concentration profiles in layer I are concentrated at Mg-10at%Al of the Mg-Al-Y ternary phase diagram. However, these concentration profiles in layer II are concentrated in Al_2Y + $\gamma(Mg_{17}Al_{12})$ + (Mg) and Al_2Y + (Mg) regions. Mg is the base of the terminal alloys, $Mg_{17}Al_{12}$ and $Mg_{24}Y_5$ exist in Mg-40Al and Mg-30Y alloys, respectively. The shape of the diffusion path is S-shaped. This agrees with the results of the diffusion path in the single-phase region reported in the literature [21]. So Al_2Y is the only newly formed phase in the diffusion path.

Figure 4 shows a schematic diagram of sample preparation process and the XRD result of the diffusion couple annealing for 72 h at 400 °C. The XRD pattern shows the existence of $Mg_{24}Y_5$ and Al_2Y phases. The $Mg_{24}Y_5$ phase already exists in the Mg-30Y matrix. The Al_2Y phases are formed by the interaction between Al and Y.

(a)　　　　　　　　　　　　　　　　　**(b)**
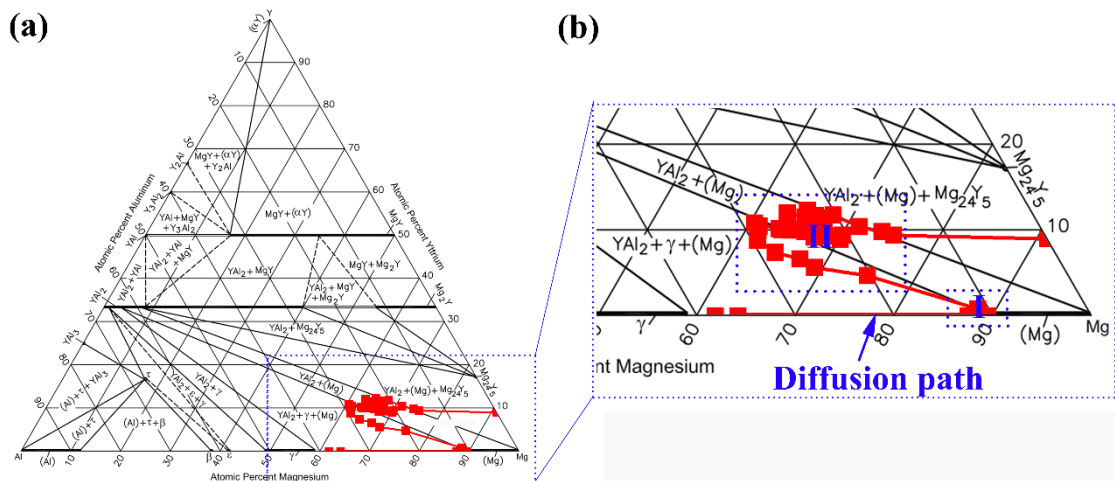
Figure 3. (**a**) The diffusion path for the diffusion couple on isothermal section at 400 °C of the Mg-Al-Y system, (**b**) a larger version of the dotted box in Figure 3a.
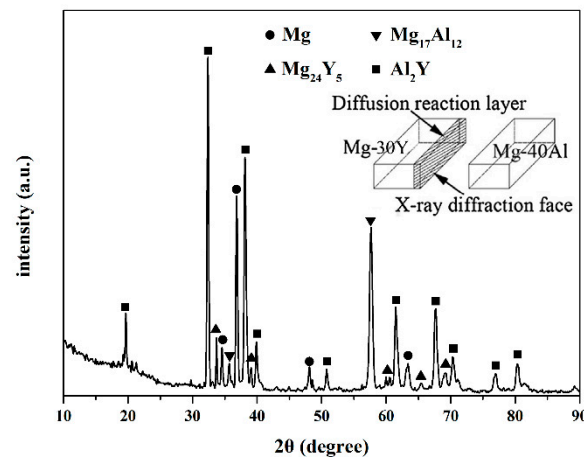
Figure 4. XRD pattern for the diffusion couple annealing for 72 h at 400 °C.

4.4. Thermodynamic Analysis

The standard enthalpy of formation (ΔH) can predict the binary alloy formation. According to the thermodynamic parameters of Mg, Al and Y in the literature [23], ΔH can be calculated using Miedema model [24]. Figure 5 shows ΔH of formation for Mg-Al, Mg-Y and Al-Y systems. It is clear that ΔH of formation for Mg-Al, Mg-Y and Al-Y systems are all negative, ΔH for Mg-Y system are closer to the Mg-Al system than the Al-Y system, and ΔH for Mg-Al and Mg-Y systems is far higher than Al-Y system. It indicates that the stable Al-Y intermetallic phases are first formed in the Mg-Al-Y system. This is consistent with the thermodynamic calculation results in the literature [9]. In addition, the Al_4MgY phase is the only ternary phase reported in the Mg-Al-Y system [22]. The melting point of the Al-Y intermetallic phases are higher than the Al_4MgY phase [8], therefore, during the existence of the Al-Y intermetallic phase in the Mg-Al-Y system, the Al_4MgY phase is difficult to form in this study.

The Gibbs energy of formation (ΔG_f) can be an effective prediction of intermetallic phase formation. Moreover, the reaction with the lowest ΔG_f tends to occur among all the possible reactions. ΔG_f of the Al-Y intermetallic phases are described by a linear function of the temperature T: $\Delta G_f = a + bT$. The thermodynamic parameters of a and b can be evaluated using phase diagram and thermodynamic data. Optimized thermodynamic parameters for the Al-Y intermetallic phases are listed in Table 1 [8]. As shown in Figure 6, ΔG_f of Al_2Y is lower than those of Al_3Y, AlY, Al_2Y_3 and AlY_2, which indicates that that Al_2Y is the most stable phase of the Al-Y system. The variation of ΔG_f for the Al-Y intermetallic phases is consistent with that reported in literature [25,26].
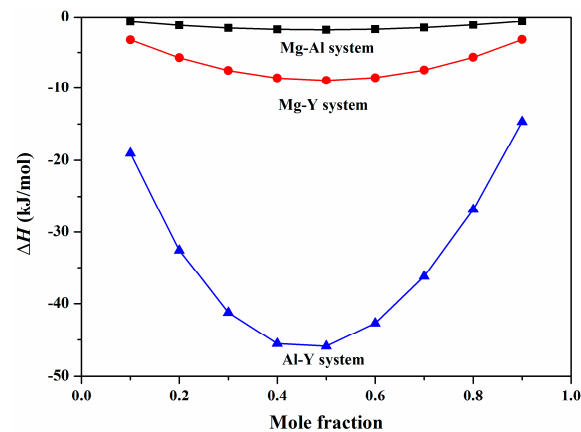
Figure 5. Standard enthalpy of formation of Mg-Al, Mg-Y and Al-Y systems.

Table 1. Optimized thermodynamic parameters for Al-Y intermetallic phases [8].

Intermetallic Phase	a (J mol^{-1})	b (J (mol K)$^{-1}$)
Al$_3$Y	$-39,727.972$	8.036
Al$_2$Y	$-50,410.046$	10.230
AlY	$-48,074.303$	11.536
Al$_2$Y$_3$	$-45,347.395$	12.364
AlY$_2$	$-38,200.000$	10.568
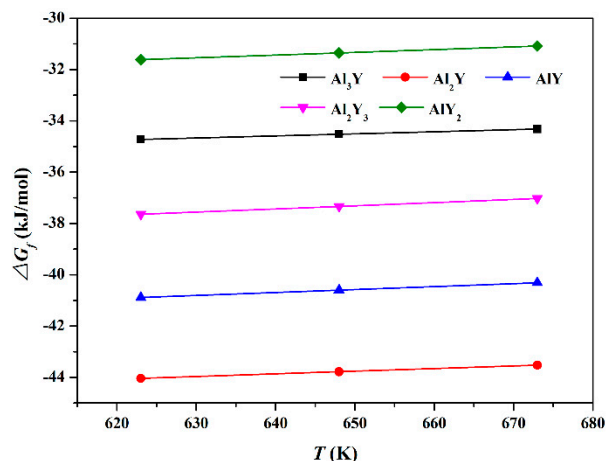
Figure 6. Gibbs energy of formation of Al-Y intermetallic phases in the temperature range of this experiment.

4.5. EDS Characterizing Intermetallic Phases

BSE images of regions 1 and 2 in Figure 1i are shown in Figure 7. In Figure 7a, it is found that after Al atoms diffused into the Mg-30Y matrix, the Al-Y compounds basically formed along the morphology of the previous Mg$_{24}$Y$_5$, which were the dense block phases of close to the Mg-40Al matrix and the acicular phase of far from the Mg-40Al matrix. In region 2, a large number of lamellar intermetallic phases are apparent. EDS point analysis was carried out to identify the composition of the reaction lay and their constituents. Table 2 lists the results of EDS analysis. Many studies in the literature have reported that Al$_2$Y is the most common Al-Y intermetallic phase in Mg alloys [3–6,27]. A Mg-Al-Y vertical section at 80 wt % Mg computed by Shakhshir et al. [8] is compared. It is found that in addition to Mg$_{24}$Y$_5$ and Mg$_{17}$Al$_{12}$, only in Al-Y intermetallic phases, Al$_2$Y, was formed at 80 wt % Mg. Combined with the EDS, diffusion path, thermodynamics analysis and XRD results, the phase composition of each point is determined and shown in Table 2.
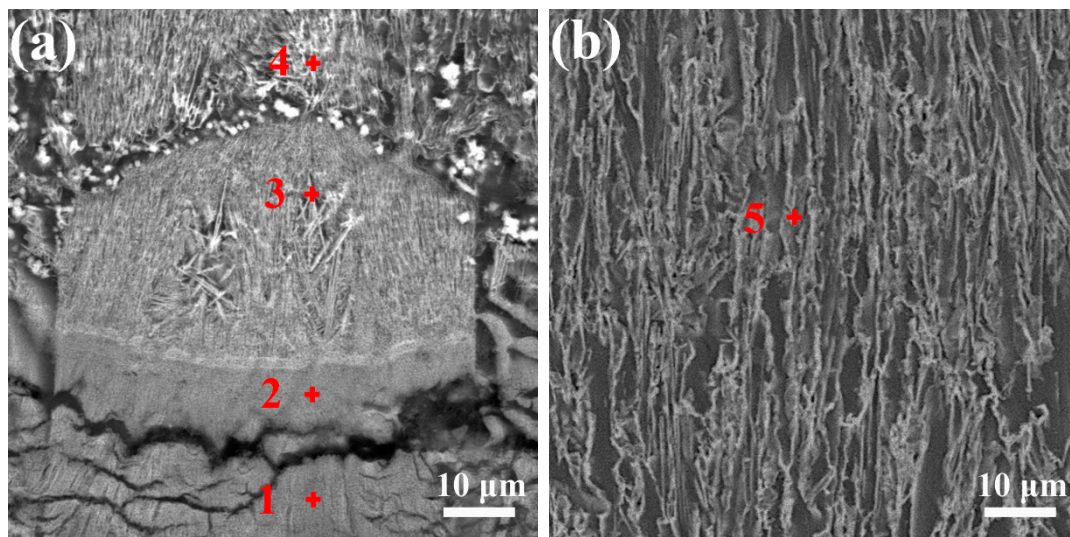
Figure 7. BSE images of (**a**) region 1 and (**b**) region 2 for the Figure 1i.

Table 2. EDS results of the reaction layer as denoted in Figure 7.

Point	Mg (at.%)	Al (at.%)	Y (at.%)	Corresponding Phase
1	74.71	20.56	4.72	$Al_2Y + \gamma + (Mg)$
2	66.87	26.42	6.71	$Al_2Y + \gamma + (Mg)$
3	60.78	28.68	10.54	$Al_2Y + (Mg)$
4	62.91	25	12.09	$Al_2Y + (Mg)$
5	65.7	22.95	11.35	$Al_2Y + (Mg)$

The line scan in Figure 8 shows that a lean Y region is formed at the end of the reaction layer near the Mg-30Y matrix. It is possible that Y in Mg-30Y matrix diffused into the reaction layer to form Al_2Y compounds. Yu et al. [28,29] showed that Y tends to diffused towards the interface.
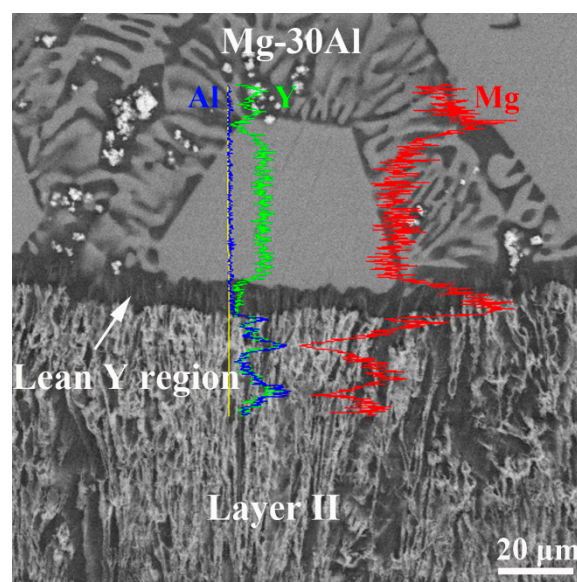

Figure 8. BSE/EDS line of the region 3 in Figure 1i.

4.6. Growth Kinetics of Reaction Layers

Figure 9 shows the thickness reaction layer plotted against the square root of time. It is found that the linear extrapolation of the experimental data intersects through the origin, which proves that

the growth constant of the reaction layer and the thickness of the diffusion layer have a parabolic trend with time. Therefore, the growth of reaction layers is controlled by diffusion mechanisms. The growth constants of the reaction layer are calculated from Equations (1) and (2). Figure 10 presents an Arrhenius plot of the reaction layers. The growth constants of the reaction layer are listed in Table 3. The magnitudes of the growth constants for the reaction layers are consistent with the previous study on the interfacial reaction of Mg alloys [17–19]. Especially at 400 °C, the growth constant of the reaction layer is $k_{(Mg-40Al)/(Mg-30Y)} > k_{(Mg-40Al)/(Mg-30Nd)} > k_{(Mg-40Al)/(Mg-20Ce)} > k_{(Mg-40Al)/(Mg-20Ca)}$. This is exactly the same as the law of the radius of Y, Nd, Ce, and Ca atoms ($r_Y > r_{Nd} > r_{Ce} > r_{Ca}$). Therefore, the growth constants of reaction layers may be related to the atomic size of alloying elements in magnesium alloys. The activation energy of the reaction layer is larger than we studied before [17–19].
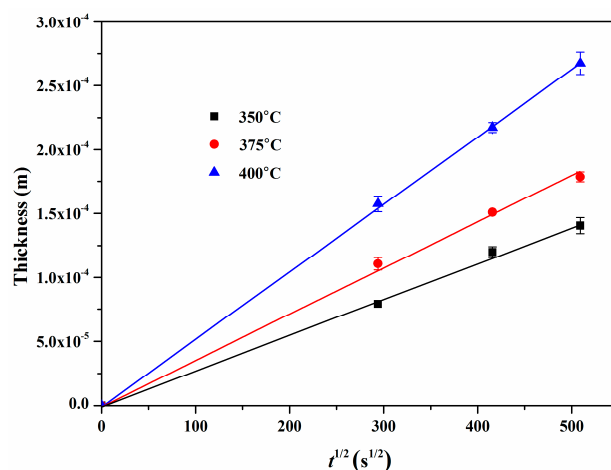

Figure 9. Thickness of reaction layer and square root of the time in the temperature range of 350–400 °C.
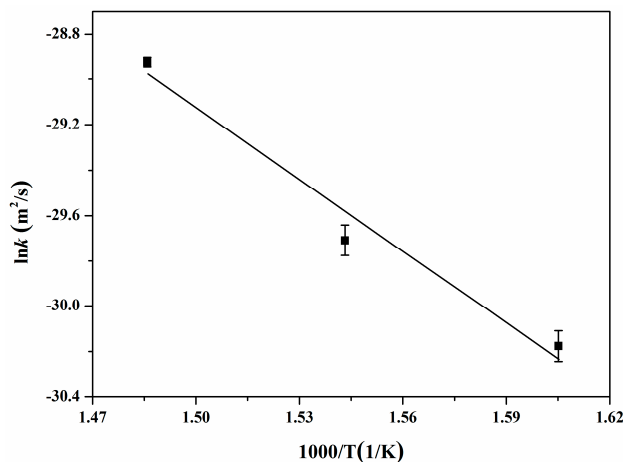

Figure 10. Growth constants for the reaction layers as a function of temperature.

Table 3. The growth constants of reaction layer of the diffusion couples.

T (°C)	k (m² s⁻¹)	k_0 (m² s⁻¹)	Q (kJ mol⁻¹)
350	$(7.84 \pm 0.13) \times 10^{-14}$		
375	$(1.25 \pm 0.08) \times 10^{-13}$	$(1.48 \pm 0.10) \times 10^{-6}$	87.09 ± 0.73
400	$(2.75 \pm 0.05) \times 10^{-13}$		

4.7. Interdiffusion Coefficients

In this study, Mg is the matrix, so the interdiffusion coefficient of Mg is not calculated. Layer I is formed by the Al element in Mg-40Al matrix diffused across the original interface to Mg-30Y matrix,

but Y in Mg-30Y matrix does not diffused to Mg-40Al matrix. However, both Al and Y diffused in layer II. Therefore, the interdiffusion coefficients of Al and Y in layer II are calculated. In addition, ΔC_i could not be determined in this study. Thus, the average effective interdiffusion coefficients were not calculated. The integrated interdiffusion coefficients, $\widetilde{D}_i^{Int,II}$, of Al and Y are calculated from Equation (4) and given in Table 4. The magnitude of $\widetilde{D}_{Al}^{Int,II}$ agree well with Brennan et al. [30] and our previous study [18]. In layer II, $\widetilde{D}_{Al}^{Int,II}$ are higher than $\widetilde{D}_{Y}^{Int,II}$, and $\widetilde{Q}_{Y}^{Int,II}$ is higher than $\widetilde{Q}_{Al}^{Int,II}$. In the solid diffusion process, the element diffusion is proportional to the melting point of the alloy and inversely proportional to the atomic radius. The melting points of Mg-30Y master alloy (595 °C) are higher than Mg-40Al master alloy (460 °C). In addition, Al (143 pm) has a smaller atomic radius than Y (227 pm). Therefore, Al atoms are more easily diffused than Y atoms in magnesium alloys.

Table 4. The diffusion parameters of the Al and Y in the layer II.

i	T (°C)	$\widetilde{D}_i^{Int,II}$ (m^2/s)	$\widetilde{D}_0^{Int,II}$ (m^2 s^{-1})	$\widetilde{Q}_i^{Int,II}$ (kJ mol^{-1})
	350	1.44×10^{-14}		
Al	375	2.98×10^{-14}	2.20×10^{-6}	97.61
	400	5.83×10^{-14}		
	350	5.13×10^{-15}		
Y	375	1.24×10^{-14}	2.40×10^{-5}	115.29
	400	2.68×10^{-14}		

5. Conclusions

1. Two sub-layers were formed in the diffusion couples at 350–400 °C. Most of the newly formed intermetallic phases in the reaction layer distribute along the morphology of Mg$_{24}$Y$_5$ before diffusion.

2. During the whole interfacial reactions process, Y in Mg-30Y matrix hardly diffused into Mg-40Al matrix, but Al from Mg-40Al matrix diffused into Mg-30Y matrix. The Al-Y intermetallic phases were formed when Al diffused into Mg-30Y matrix. Diffusion path, XRD, thermodynamics analysis and EDS results show that Al$_2$Y is the only newly formed phase at the interface of diffusion couple.

3. The growth of reaction layers is controlled by diffusion mechanisms. The diffusion activation energy for the reaction layers is calculated to be (87.09 ± 0.73) kJ/mol. The $\widetilde{D}_{Al}^{Int,II}$ are higher than $\widetilde{D}_{Y}^{Int,II}$ in the temperature range of 350–400 °C. The diffusion activation energy of Y is higher than that of Al.

References

1. Karakulak, E. A review: Past, present and future of grain refining of magnesium castings. *J. Magnes. Alloy.* **2019**, *7*, 355–369. [CrossRef]

2. Song, J.; She, J.; Chen, D.; Pan, F. Latest research advances on magnesium and magnesium alloys worldwide. *J. Magnes. Alloy.* **2020**, *8*, 1–41. [CrossRef]

3. Qiu, D.; Zhang, M.-X. The nucleation crystallography and wettability of Mg grains on active Al$_2$Y inoculants in an Mg-10 wt% Y Alloy. *J. Alloys Compd.* **2014**, *586*, 39–44. [CrossRef]

4.　Qiu, D.; Zhang, M.-X.; Kelly, P.M. Crystallography of heterogeneous nucleation of Mg grains on Al$_2$Y nucleation particles in an Mg-10 wt.% Y alloy. *Scr. Mater.* **2009**, *61*, 312–315. [CrossRef]

5.　Chang, H.-W.; Qiu, D.; Taylor, J.; Easton, M.; Zhang, M.-X. The role of Al$_2$Y in grain refinement in Mg-Al-Y alloy system. *J. Magnes. Alloy.* **2013**, *1*, 115–121. [CrossRef]

6.　Jiang, Z.; Feng, J.; Chen, Q.; Jiang, S.; Dai, J.; Jiang, B.; Pan, F. Preparation and Characterization of Magnesium Alloy Containing Al$_2$Y Particles. *Materials* **2018**, *11*, 1748. [CrossRef]

7.　Tang, Q.; Sun, H.; Zhou, M.; Quan, G. Effect of Y Addition on the Semi-Solid Microstructure Evolution and the Coarsening Kinetics of SIMA AZ80 Magnesium Alloy. *Metals* **2017**, *7*, 416. [CrossRef]

8.　Shakhshir, S.A.; Medraj, M. Computational thermodynamic model for the Mg-Al-Y system. *J. Ph. Equilib. Diffus.* **2006**, *27*, 231–244. [CrossRef]

9.　Huang, W.; Yan, H. Calculation of thermodynamic parameters of Mg-Al-Y alloy. *J. Wuhan Univ. Technol.* **2014**, *29*, 374–378. [CrossRef]

10.　Drits, M.E.; Padezhnova, E.M.; Dobatkina, T.V. Phase Equilibria in Magnesium-Yttrium-Aluminum Alloys. *Metall* **1979**, *3*, 223–227.

11.　Zarechnyuk, O.S.; Drits, M.E.; Rykhal, R.M.; Kinzhibalo, V.V. Examination of the Mg-Al-Y System (0-33 at% Y) at 400 °C. *Metall* **1980**, *5*, 242–244.

12.　Odinev, K.O.; Ganiev, I.N.; Kinzhibalo, V.V.; Kurbanov, K.K. Phase Equilibria in Aluminum-Magnesium-Yttrium and Aluminum-Magnesium-Cerium Systems at 673 K. *Tsvetn. Metall* **1989**, *4*, 75–77.

13.　Das, S.K.; Kim, Y.; Ha, T.; Gauvin, R.; Jung, I.-H. Anisotropic Diffusion Behavior of Al in Mg: Diffusion Couple Study Using Mg Single Crystal. *Metall. Mater. Trans. A* **2013**, *44*, 2539–2547. [CrossRef]

14.　Das, S.K.; Kang, Y.-B.; Ha, T.; Jung, I.-H. Thermodynamic modeling and diffusion kinetic experiments of binary Mg-Gd and Mg-Y systems. *Acta Mater.* **2014**, *71*, 164–175. [CrossRef]

15.　Dayananda, M.A. An analysis of concentration profiles for fluxes, diffusion depths, and zero-flux planes in multicomponent diffusion. *Metall. Mater. Trans. A* **1983**, *14*, 1851–1858. [CrossRef]

16.　Dayananda, M.A. Average effective interdiffusion coefficients and the Matano plane composition. *Metall. Mater. Trans. A* **1996**, *27*, 2504–2509. [CrossRef]

17.　Dai, J.; Jiang, B.; Li, X.; Yang, Q.; Dong, H.; Xia, X.; Pan, F. The formation of intermetallic phases during interdiffusion of Mg-Al/Mg-Ce diffusion couples. *J. Alloys Compd.* **2015**, *619*, 411–416. [CrossRef]

18.　Dai, J.; Shen, S.; Jiang, B.; Zhang, J.; Yang, Q.; Jiang, Z.; Dong, H.; Pan, F. Interfacial reaction in (Mg-37.5Al)/(Mg-6.7Nd) diffusion couples. *Met. Mater. Int.* **2016**, *22*, 1–6. [CrossRef]

19.　Dai, J.; Xiao, H.; Jiang, B.; Xie, H.; Peng, C.; Jiang, Z.; Zou, Q.; Yang, Q.; Pan, F. Diffusion behavior and reactions between Al and Ca in Mg alloys by diffusion couples. *J. Mater. Sci. Technol.* **2018**, *34*, 291–298. [CrossRef]

20.　Kirkaldy, J.S.; Brown, L. Diffusion behaviour in ternary, multiphase systems. *Can. Metall. Quart.* **1963**, *2*, 89–115. [CrossRef]

21.　Morral, J.E. Diffusion path theorems for ternary diffusion couples. *Metall. Mater. Trans. A* **2012**, *43*, 3462–3470. [CrossRef]

22.　Raghavan, V. Al-Mg-Y (aluminum-magnesium-yttrium). *J. Ph. Equilib. Diff.* **2007**, *28*, 477–479. [CrossRef]

23.　De Boer, F.R.; Boom, R.; Mattens, W.C.M.; Miedema, A.R.; Niessen, A.K. *Cohesion in Metals: Transition Metal Alloys*; Elsevier: Amsterdam, The Netherlands, 1988.

24.　Miedema, A.; De Chatel, P.; De Boer, F. Cohesion in alloys-fundamentals of a semi-empirical model. *Physica B + C* **1980**, *100*, 1–28. [CrossRef]

25.　Liu, S.; Du, Y.; Chen, H. A thermodynamic reassessment of the Al-Y system. *Calphad* **2006**, *30*, 334–340. [CrossRef]

26.　Ran, Q.; Lukas, H.L.; Effenberg, G.; Petzow, G. A thermodynamic optimization of the Al-Y system. *J. Less Common Met.* **1989**, *146*, 213–222. [CrossRef]

27.　Peng, Z.Z.; Shao, X.H.; Guo, X.W.; Wang, J.; Ma, X.L. Atomic-Scale Insight into Structure and Interface of Al$_2$Y Phase in an Mg-Al-Y Alloy. *Adv. Eng. Mater.* **2018**, *20*. [CrossRef]

28.　Yu, X.; Jiang, B.; Yang, H.; Yang, Q.; Xia, X.; Pan, F. High temperature oxidation behavior of Mg-Y-Sn, Mg-Y, Mg-Sn alloys and its effect on corrosion property. *Appl. Surf. Sci.* **2015**, *353*, 1013–1022. [CrossRef]

29. Yu, X.; Jiang, B.; He, J.; Liu, B.; Jiang, Z.; Pan, F. Effect of Zn addition on the oxidation property of Mg-Y alloy at high temperatures. *J. Alloys Compd.* **2016**, *687*, 252–262. [CrossRef]

30. Brennan, S.; Bermudez, K.; Kulkarni, N.S.; Sohn, Y. Interdiffusion in the Mg-Al System and Intrinsic Diffusion in β-Mg$_2$Al$_3$. *Metall. Mater. Trans. A* **2012**, *43*, 4043–4052. [CrossRef]